Synthesis and Characterization of Cobalt(II)–Iron(III) Hydroxide Carbonate, a Layered Double Hydroxide Belonging to the Pyroaurite Group

Hans Christian Bruun Hansen[1]

Chemistry Department, Royal Veterinary & Agricultural University, Thorvaldsensvej 40, DK-1871 Frederiksberg C., Copenhagen, Denmark

Christian Bender Koch

Physics Department, Bld. 307, Technical University of Denmark, DK-2800 Lyngby, Denmark

and

Reginald Morton Taylor

CSIRO Division of Soils, Private Bag 2, Glen Osmond, South Australia, Australia

A pure pyroaurite-type compound (PTC) with the composition $[Co_{5.42}^{II}Fe_{2.47}^{III}(OH)_{16}][(CO_3)_{1.12}xH_2O]$ ($x = 5$–6) has been synthesized by air oxidation of Fe(II) in a solution of $Co(NO_3)_2$ at pH 6.60 and has been characterized by powder X-ray diffraction, electron microscopy, Fourier transform infrared spectroscopy, Mössbauer spectroscopy, and differential thermal analysis. This reddish-brown compound consists of mostly hexagonally shaped crystals (diam. 0.1–0.4 μm) apparently more or less intergrown and forming spherical aggregates (diam. 3–5 μm). The hexagonal unit-cell parameters are $a = 0.312$ and $c = 2.278$ nm, and there is an ordered stacking of consecutive hydroxide layers. On heating in a nitrogen atmosphere, two DTA endothermic peaks are observed at 195 and 260°C, respectively; the low-temperature peak is due to desorption of interlayer water, whereas decomposition of carbonate and dehydroxylation of the structure causes the high-temperature peak. Mössbauer parameters ($\delta = 0.35$ mm s^{-1} and $\Delta E_Q = 0.49$ mm s^{-1} at 298 K) are consistent with ferric ions in the high spin state. From the IR spectrum, the D_{3h} symmetry of the interlayer CO_3^{2-} appears unperturbed. © 1994 Academic Press, Inc.

INTRODUCTION

Increasing interest is being paid to the layered double metal hydroxides of the pyroaurite–sjögrenite group (pyroaurite type compounds, PTCs). This interest stems from their possible role as important intermediates in natural mineral transformations and geochemical processes,

and also from their technical applications as anion exchangers, adsorbents, molecular sieves, and catalysts (1–8). The structural units of the pyroaurite type compounds comprises positively charged trioctahedral metal hydroxide layers which alternate with charge compensating layers of anions and water (9, 10) (see Fig. 1). A generalized formula is $[M_{a(8-x)}^{II}M_{bx}^{III}(OH)_{16}]$ $[(A^{n-})_{x/n}yH_2O]$, with M_a = Mg, Zn, Fe, Co, Ni, Cu, Cd, Mn; M_b = Al, Fe, Cr, Mn, Co, Ni, Sc, Ga; and A^{n-} is an anion which does not form strong complexes with either M_a or M_b cations. For natural well-crystalline carbonate forms the amount of interlayer water (y) has been found in the range 4–5 (11–13). Ratios of $M_a : M_b$ normally are reported to be in the range 2–3. In the following, specific PTCs will be denoted by the element symbols for M_a and M_b in front of "PTC." PTCs with the same combination of M_a and M_b but different anions in the interlayer will be described as anion "forms."

Pyroaurite group compounds normally are synthesized by precipitation of a solution of M_a- and M_b-salts with base (normally NaOH, KOH, or NH$_3$), or a solution of metal salt and a solid hydroxide or oxide of either M_a or M_b is used as reactants. If no precautions are taken to exclude CO$_2$ from the system carbonate forms are synthesized. Normally these are the most crystalline and may be used as starting materials for preparing other anionic forms (3, 14, 15). The precipitation may be carried out at high pH by mixing the solution of the di- and trivalent metal salts with an excess of strong base. However in
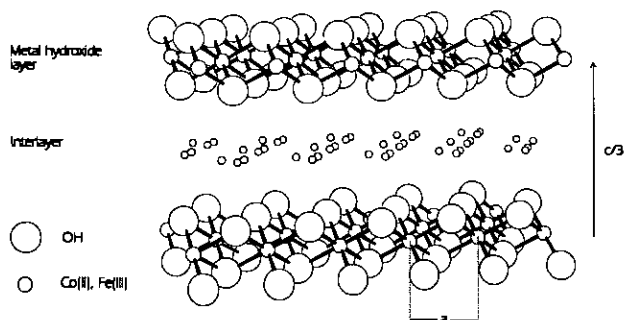
[1] E-mail: kvlxhaha@uts.uni-c.dk.

FIG. 1. Structure of pyroaurite type compounds consisting of tri-octahedral metal hydroxide layers alternating with layers of anions and water molecules (only oxygen sites shown). The layers are perpendicular to the c-axis. Drawing based on data from Allmann (11, 12).

many cases the precipitation is carried out at fixed pH or a final maximum pH is achieved. Taylor and McKenzie (16) developed a constant-pH precipitation method called "induced hydrolysis" by which a freshly precipitated hydroxide of the trivalent metal at fixed pH was reacted with a metal salt solution of the divalent metal at the same pH. Hansen and Taylor (17, 18) developed other constant-pH precipitation methods by which well crystallized carbonate forms of MgFe(III)-PTC and MgMn(III)-PTCs could be synthesized by air oxidation of Fe(II) or Mn(II), respectively, in aqueous solutions of salts of the divalent metal cations (M_a). By use of these methods PTCs without extensive stacking disorder of consecutive hydroxide layers could be synthesized in contrast to products from rapid precipitation at alkaline pH (17–19). Crystallite size has been reported to increase by hydrothermal treatments of the rapidly formed precipitates (20). However, single crystals bigger than approximately 20 μm in diameter has apparently never been prepared.

The Fe(II)Fe(III)-PTC (green rust) plays an important role as a solid intermediate when solutions containing Fe(II) are oxidized around neutrality or when iron corrodes. On oxidation the green rust may transform into magnetite (Fe_3O_4), maghemite $(\gamma\text{-}Fe_2O_3)$, lepidocrocite $(\gamma\text{-}FeOOH)$, feroxyhite $(\delta\text{-}FeOOH)$ or goethite $(\alpha\text{-}FeOOH)$ the exact transformation being governed by variables like pH, oxidation rate, and anions present (21–28). These transformations have been claimed to be topotactic (29), but are very fast and hence difficult to investigate. However a few other PTCs containing easy oxidizable divalent cations (e.g., Mn(II) or Co(II)) together with Fe(III) may be synthesized. Co(III) is known for its substitution inertness. Hence the solid state oxidation of Co(II) to Co(III) in a PTC compound may lead to kinetically stable structural intermediates. Oxidation studies of Co(II) Fe(III)-PTC could be of help in interpretation of the structural reorganisations of the octahedral metal hydroxide

layer following an increase in the oxidation state of the M_a cation, changes which may be very similar to those occuring when green rust is oxidized.

Few attempts on the synthesis of Co(II)Fe(III)-PTCs have been reported. Feitknecht (30) synthesized the chloride form by coprecipitation. However the product also contained impurities of $Co(OH)_2$. The chloride form was prepared by Petit (31) by the electrochemical oxidation of Co–Fe anodes in solutions of NaCl at pH 7. Taylor (23) prepared the carbonate form of the Co(II)Fe(III)PTC by the induced hydrolysis method. None of these studies comprised chemical, thermal, and spectroscopic analyses of the products.

We report here on a new method for the synthesis of a rather well crystalline carbonate form of Co(II)Fe(III)-PTC. The product has been characterized by X-ray diffraction (XRD), chemical analysis, scanning and transmission electron microscopy (SEM, TEM), Fourier transform infrared spectroscopy (FTIR), thermogravimetric and differential thermal analysis (TGA, DTA), and Mössbauer spectroscopy.

EXPERIMENTAL

Synthesis

The syntheses were carried out in a cylindrical (diam., 77 mm; height, 150 mm), thermostatted (35°C) glass vessel fitted with an air-tight lid and with magnetic stirring of the solution. Four hundred cm^3 0.1 M $Co(NO_3)_2 \cdot 6H_2O$ in the vessel was bubbled with nitrogen (30 $cm^3 \cdot min^{-1}$) for two hours before addition of 8.0 mmole of $FeCl_2 \cdot 4H_2O$. The pH was adjusted to 6.60 before air oxidation commenced (0.62 $cm^3 \cdot min^{-1}$). During oxidation pH was kept constant at 6.60 by the addition of 0.5 M $NaHCO_3$ controlled by a pH-stat. The carbon dioxide produced during titration was expelled by the continued bubbling of nitrogen (30 $cm^3 \cdot min^{-1}$) through the suspension. When addition of alkali ceased due to oxidation of all Fe(II) to Fe(III) the reddish-brown precipitate was separated by centrifugation and washed with water until the conductivity of the supernatant was below 20 μS. The final product was dried at 60°C for 5 h. Synthesis at pH 6.60 was found to be optimal, as product crystallinity and/or purity decreased when working at either lower or higher pH values.

Chemical Composition

The content of metals, hydroxide and carbonate was determined as previously described (17). The oxidation state of cobalt was determined by dissolving the compound in 1 M HCl, distilling the liberated Cl_2 into a KI solution and titrating the I_2 formed with 0.01 M $Na_2S_2O_3$.

X-Ray Diffraction

Samples as unoriented powders were scanned from 6–80°2Θ at 1°2Θ min⁻¹ using Co $K\alpha$ radiation. Quartz was used as internal standard. Unit cell constants were calculated using a least squares refinement. Powder XRD traces were simulated using POWD10 (32) using the atomic positions given by Allmann (11, 12), and assuming an equidimensional crystallite size of 50 nm.

Scanning Electron Microscopy/Transmission Electron Microscopy

Scanning electron micrographs (SEM) were obtained using a JEOL JSM-U3 instrument operated at 25 kV and Pt-coating of the sample. Transmission electron micrographs (TEM) were obtained using a Philips EM 430 microscope operated with an acceleration voltage of 300 kV, and particles dispersed using ultrasonic bath and placed on a holey carbon grid. The TEM is equipped with an EDAX energy dispersive X-ray detector (EDX).

Fourier Transform Infrared Spectroscopy

Transmission spectra were recorded on a Perkin–Elmer 2000 FT-spectrometer at a resolution of 2 cm⁻¹ and averaging over 20 scans in the 4000–450 cm⁻¹ region (MIR) and 50 scans in the 450–100 cm⁻¹ region (FIR). For the MIR 1 mg of sample was mixed with 200 mg of KBr in a mortar and pressed at 8 tons before examination. In the FIR KBr were replaced with polyethylene powder as the diluting agent.

Thermal Analysis

Differential thermal analysis (DTA) with simultaneous detection of the water and carbon dioxide liberated was carried out using a Stanton Redcroft 673-4 DTA apparatus mounted with IR detectors for water and carbon dioxide (33). Pure nitrogen was used as the carrier gas.

Mössbauer Spectroscopy

⁵⁷Fe Mössbauer spectra were obtained at 298, 80, and 12 K using a constant acceleration Mössbauer spectrometer and a Co in Rh source. The spectrometer was calibrated using a thin foil of α-Fe at room temperature and isomer shifts are given relative to the centroid of the spectrum of this absorber.

RESULTS AND DISCUSSION

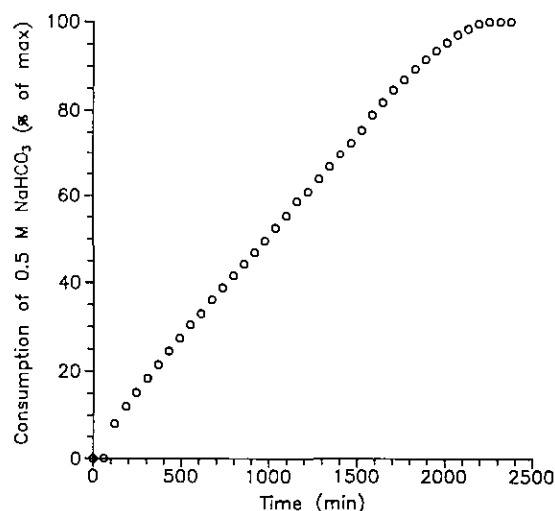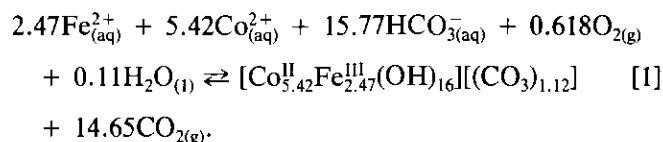A typical titration curve obtained during the oxidation of Fe(II) in a solution of Co(NO₃)₂ at constant pH (6.60)

FIG. 2. Synthesis of Co(II)Fe(III)-PTC. Relative consumption of 0.5 M NaHCO₃ during air oxidation of 0.02 M Fe²⁺ in solution of 0.1 M Co(NO₃)₂ at constant pH 6.60. Oxygenation was started just following the second data point.

is shown in Fig. 2. The overall reaction for the synthesis may be formulated as (using the stochiometry of the product given in Table 1)

$$2.47Fe^{2+}_{(aq)} + 5.42Co^{2+}_{(aq)} + 15.77HCO^-_{3(aq)} + 0.618O_{2(g)}$$

$$+ 0.11H_2O_{(l)} \rightleftarrows [Co^{II}_{5.42}Fe^{III}_{2.47}(OH)_{16}][(CO_3)_{1.12}] \quad [1]$$

$$+ 14.65CO_{2(g)}.$$

From the titration curve the rate of formation of Co(II)Fe(III)-PTC is seen to be constant; apparently, the reaction is zero order. Fe³⁺ (or hydroxy complexes thereof), whence formed, must react rapidly with Co²⁺, OH⁻, and CO₃²⁻ to precipitate Co(II)Fe(III)-PTC. This conclusion is corroborated by the absence of iron oxide phases in the precipitate (see below). The rate of formation of PTC could depend on the concentration of Co²⁺, OH⁻, and CO₃²⁻, the concentration of which is held almost constant during the reaction. The change in concentration of Fe²⁺ is proportional with the consumption of NaHCO₃ showing that the reaction order is also zero with respect to Fe²⁺.

TABLE 1

Chemical Composition of Co(II)Fe(III)-PTC

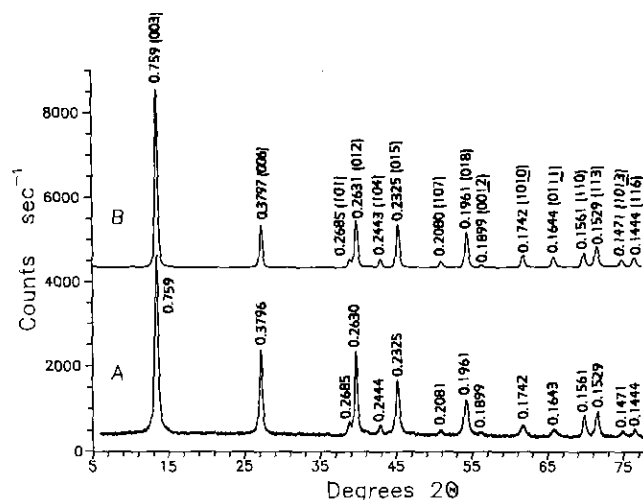| Analysis	Mass (mg)	CO₂	Fe	Co	Calc. composition
		(μmole)			
1	40.50	50.09	111.03	243.7	[Fe₂.₄₇Co₅.₄₁(OH)₁₆][(CO₃)₁.₁₁]
2	41.05	51.85	112.54	247.03	[Fe₂.₄₇Co₅.₄₃(OH)₁₆][(CO₃)₁.₁₃]

FIG. 3. X-ray diffraction traces of Co(II)Fe(III)-PTC: (A) experimental; (B) calculated. (Co K_α radiation.) d-spacings in nm. Indices refer to a hexagonal cell (a = 0.312 nm, c = 2.278 nm).

The rate of oxidation of Fe^{2+} by O_2 in aqueous solution follows the expression (34)

$$\frac{d[Fe^{2+}]}{dt} = k \cdot [Fe^{2+}] \cdot [OH^-]^2 \cdot P_{O_2}. \qquad [2]$$

In the synthesis of Co(II)Fe(III)-PTC the concentration of OH^- and O_2 is held almost constant and hence the rate of oxidation of Fe^{2+} would be expected to be of first order in Fe^{2+}. The fact that this is not found demonstrates that the mechanism of oxidation of Fe^{2+} is influenced by the presence of Co^{2+} and/or the PTC. Hence Co(II) must be assumed to actively participate, either in solution or in the PTC, in the oxidation of Fe^{2+}. Assuming the PTC surface to take part in the oxidation and assuming the surface area to be proportional with the amount of PTC formed, a rate expression,

$$\frac{d[Fe^{2+}]}{dt} = k \cdot [Fe^{2+}] \cdot [Co(II)Fe(III) - PTC], \qquad [3]$$

would result in a reaction order of zero at constant pH and concentration of O_2 because the concentration of Fe^{2+} would decrease at the same rate as Co(II)Fe(III)-PTC would be formed. In an analogous synthesis of the carbonate form of Ni(II)Fe(III)-PTC the expected first order reaction with respect to oxidation of Fe^{2+} was observed (35).

The cobalt(II)-iron(III) hydroxide carbonate is a well-crystalline PTC as evidenced by XRD (Fig. 3). All diffractions may be indexed on a hexagonal cell having a = 0.312 and c = 2.278 nm (Fig. 3). Assuming the number of interlayer water per formula unit to equal 4.5, D_x is

calculated to 2.84 g cm^{-3}. The calculated pattern approximates to the experimental pattern rather closely indicating the PTC structure model to be essentially correct for the compound. Compared with PTCs containing light metal atoms in the hydroxide layer, e.g., Al and Mg, PTCs with more heavy atoms, e.g., Co and Fe, and hence higher scattering factors give easy distinguishable 101, 104, 107, and 0012 diffraction peaks. There is no indication of severe faulting in the stacking of hydroxide layers (turbostratic disorder (19)) as nonbasal reflections are not very broad or asymmetric. An attempt to improve crystallinity by hydrothermal treatment at 100°C failed due to transformation of the hydroxide into a black Co–Fe oxide as also described by Tseung and Goldstein (36).

SEM micrographs show aggregates (diam. 3–5 μm) of platy particles (Fig. 4A) of average diameter between 0.1 and 0.4 μm and thickness of approximately 0.03 μm. Edges appear slightly serrated. Some of the particles appear to be slightly curved possibly due to the presence of screw dislocations. Sharp hexagonally outlines appear rare in SEM, but was observed in TEM (Fig. 4B). However, crystals with obtuse angles exist. Individual crystals of the open aggregates are held together partly by interparticle forces, partly by orthogonal crystal intergrowth (Fig. 4B). Pitting of crystals observed by TEM is ascribed to decomposition caused by the electron beam producing holes through which CO_2 has escaped (20).

At all temperatures the Mössbauer spectrum exhibits an asymmetric paramagnetic doublet (the 12 K spectrum is shown in Fig. 5). The spectra were fitted to one Lorentzian-shaped doublet of equal intensity and the resulting parameters are given in Table 2. These data are consistent with all the iron being present as Fe(III) in the high-spin state, as expected when oxygen is the ligand. No trace of a magnetically split sextet due to ferric oxides can be detected indicating that all the iron is within the PTC structure. The asymmetry in the spectra is probably caused by local variations in nearest cation neighbours. Small variations in the temperature dependence in isomer shift of the different sites may explain the apparent increase in linewidth when using only one doublet for fitting.

Both from XRD, microscopy and Mössbauer spectroscopy the product appears monophasic. The average formula of the compound is $[Co_{5.42}^{II}Fe_{2.47}^{III}(OH)_{16}][(CO_3)_{1.12}]$ (Table 1). The Co(II) : Fe(III) ratio is 2.19 and the OH : {Co(II) + Fe(III)} ratio is 2.03, which is close to the ideal ratio of 2 for trioctahedral metal hydroxides. No Co(III) could be detected. Analysis of individual particles using EDX-TEM yielded an average Co : Fe ratio of 2.16 with only minor variation. The mole number of water per formula unit determined indirectly as the difference between the sample weight and the sum of masses of Co, Fe, OH, and CO_3^{2-} is 5.76. If all the water is accomodated in the interlayer this implies that more than one oxygen site per
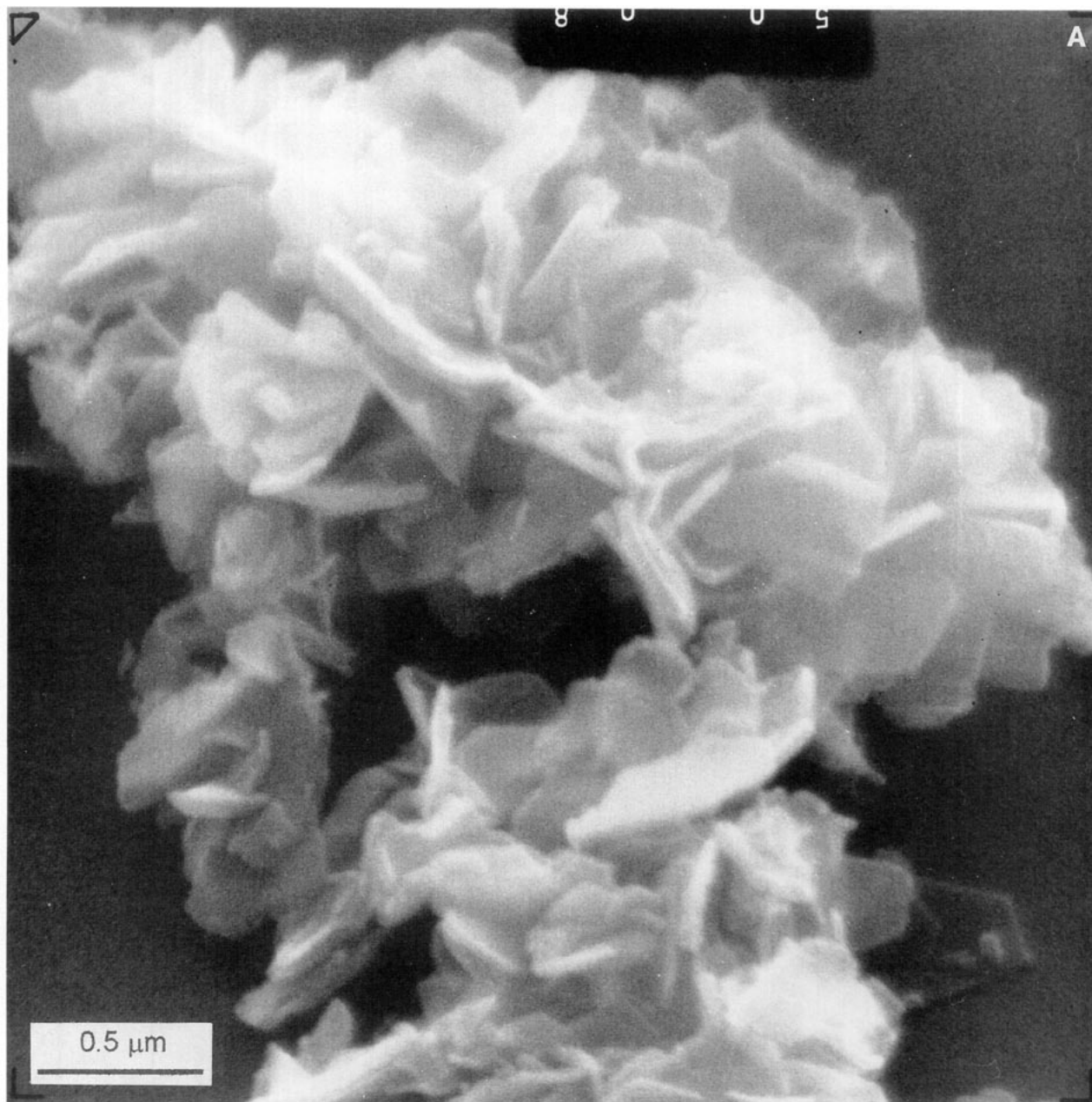
FIG. 4. Morphology of the Co(II)Fe(III)-PTC: (A) scanning electron micrograph of an aggregate of single crystals; (B) transmission electron micrograph of crystals with predominantly hexagonal outline.

group of sites has to be occupied, which should give rise to much repulsion between nearest neighbour oxygen atoms belonging to either water or carbonate ions. Hence part of the water is present outside the interlayer, probably being adsorbed in the pores of the aggregates.

On heating in N_2 two distinct endotherms are observed at 195 and 260°C, respectively (Fig. 6). Both of these endotherms are accompanied by the liberation of equal amounts of water whereas CO_2 is mostly evolved during the second endothermic reaction. Very small amounts of water and CO_2 is also given off up to a temperature of around 550°C. For pyroaurite and hydrotalcite (M_a = Mg; M_b = Fe, Al) the first endotherm is attributed to loss of interlayer water (37) and the second to loss of interlayer carbonate and structural water through dehydroxylation of the hydroxide layer (38). Also in the case of Co(II) Fe(III)-PTC, CO_2 is mainly liberated during the second endotherm. During heating the Co(II)Fe(III)-PTC decom-
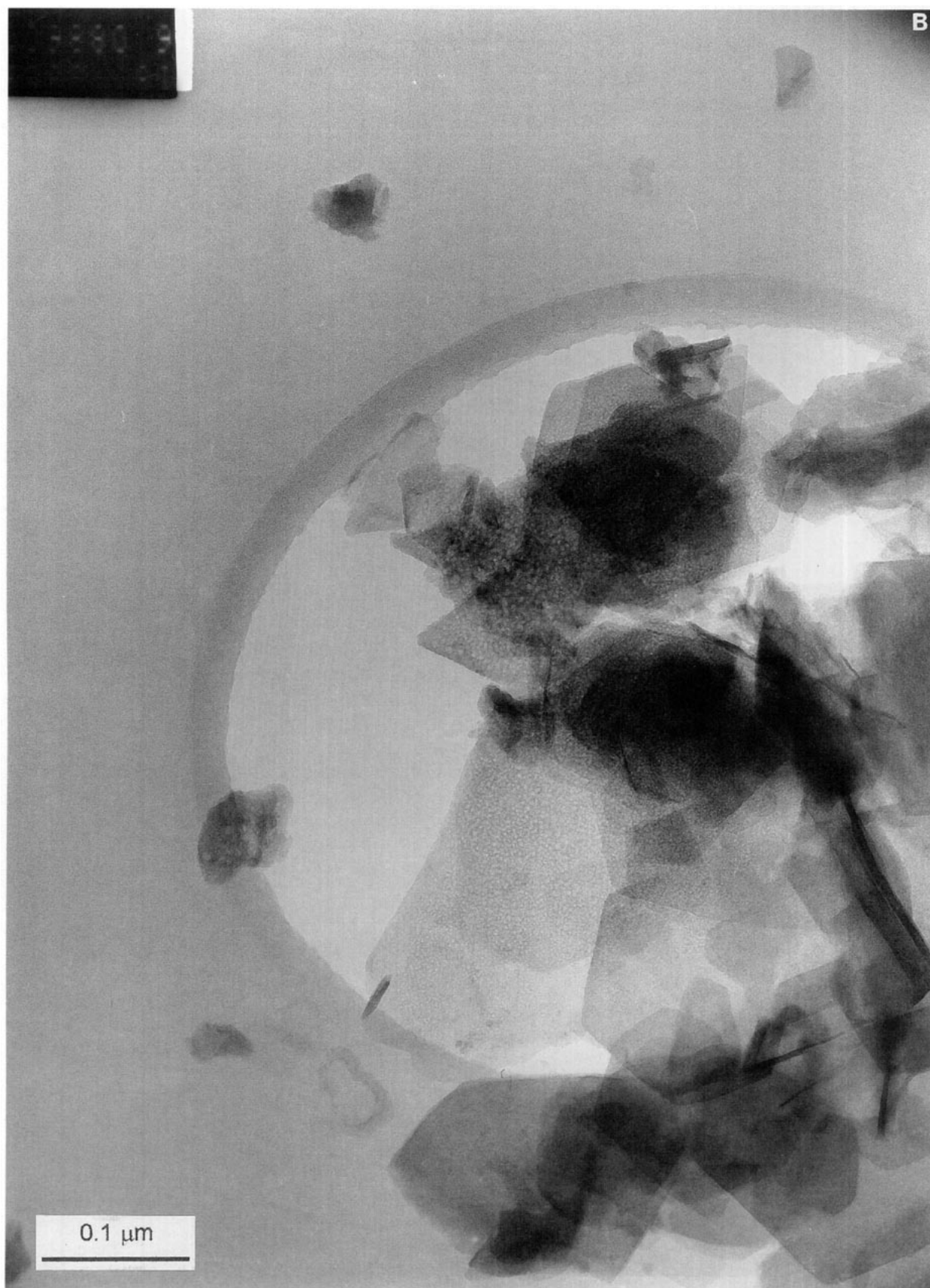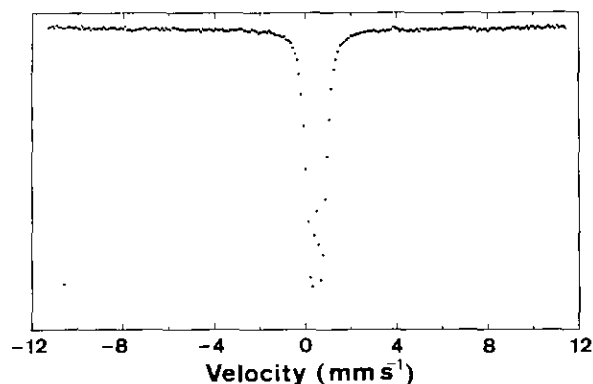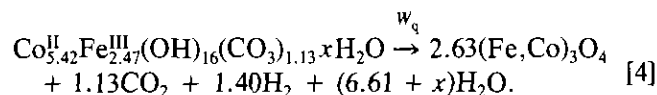
0.1 μm

FIG. 4.—*Continued*

FIG. 5. ^{57}Fe-Mössbauer spectrum of Co(II)Fe(III)-PTC obtained at 12 K.

FIG. 6. DTA curve together with water and CO_2 loss curves for Co(II)Fe(III)-PTC heated in nitrogen atmosphere.

poses starting at 115°C in static temperature heating experiments (39) analogue to reactions observed for a Co(II)Al-PTC (40). Assuming all Co(II)Fe(III)-PTC to be transformed into spinel during heat treatment, the overall reaction is expected to be

$$Co_{5.42}^{II}Fe_{2.47}^{III}(OH)_{16}(CO_3)_{1.13}xH_2O \xrightarrow{W_q} 2.63(Fe,Co)_3O_4 \\ + 1.13CO_2 + 1.40H_2 + (6.61 + x)H_2O. \quad [4]$$

Assuming the explanation for the DTA events of pyroaurite and hydrotalcite to hold also for Co(II)Fe(III)-PTC, x in equilibrium [4] is equal to 5.4 ($= 6.61 \cdot 0.45/0.55$) as the ratio of loss of interlayer water to the total water loss is 0.45 (Fig. 6). This is in good agreement with the content of water calculated from chemical data. The temperatures at which losses of interlayer water and dehydroxylation occurs from Co(II)Fe(III)-PTC is at the lower end of the temperature ranges (180–280 and 300–480°C, respectively) observed for PTCs in dynamic heating experiments when the M_a and M_b cations are not easy oxidizable (3, 17, 18, 37, 38, 41–44). For the carbonate form of a

Co(II)Al-PTC heated in nitrogen the two DTA peaks were observed at 230 and 272°C, respectively (40). The intensity of endotherm I to endotherm II is much higher for Co(II)-Fe(III)-PTC than for most other PTCs indicating the enthalpy of the dehydroxylation step to be relatively small. The stability of the Co(II, III)–Fe(III) spinel phases apparently makes the Co(II)Fe(III)-PTC a labile compound even under an inert atmosphere. This makes its use for study of the PTC spinel phase transitions quite interesting.

An FTIR spectrum of the Co(II)Fe(III)-PTC is shown in Fig. 7. The OH stretching band at 3445 cm^{-1} agrees with the patterns for other PTCs having $M_a : M_b$ ratios around 2 (45). However a shoulder at 3010 cm^{-1} does indicate the presence of a second type of OH stretching, probably due to hydrogen-bonding in the interlayer. The

TABLE 2
Mössbauer Parameters for Co(II)Fe(III)-PTC

Temp. (K)	δ	ΔE_Q	Γ
	(mm sec^{-1})		
298	0.35	0.49	0.37
80	0.46	0.51	0.40
12	0.47	0.50	0.44

Note. δ, isomer shift; ΔE_Q, quadrupole splitting; Γ, width at half height. Uncertainties on numerical values are smaller than 0.02 mm sec^{-1}.
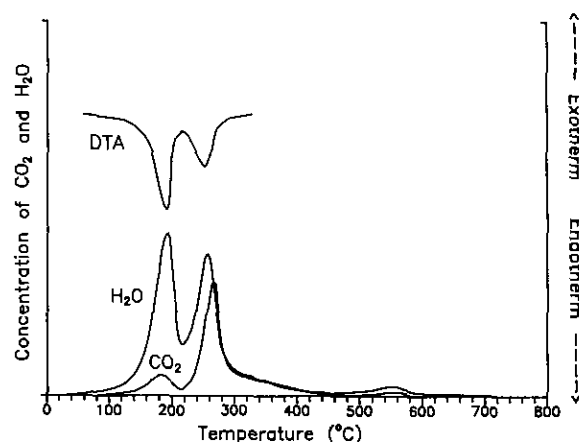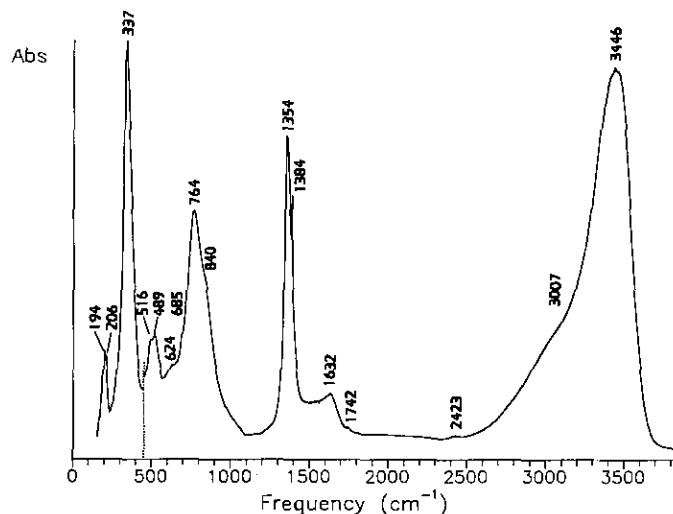

FIG. 7. FTIR transmission spectrum of Co(II)Fe(III)-PTC. (Shift of gratings and sample at 450 cm^{-1} indicated by punctured line.)

high content of interlayer water is expected to increase the intensity of interlayer hydrogen-bonding. The peak at 1632 cm^{-1} is assigned to the bending motion of interlayer water. In hydrotalcite this peak has also been assigned to HCO_3^- (46). However, after shaking the Co(II)Fe(III)-PTC with 0.1 M Na_2CO_3 for 24 hr to exchange a possible content of HCO_3^- with CO_3^{2-}, the frequency or relative intensity of this peak were unchanged. The intense absorption band at 1354 cm^{-1} and the shoulders at 840 and 685 cm^{-1} may be attributed to the CO_3^{2-} ν_3, ν_2, and ν_4 absorptions, respectively. The weak absorption at 1742 cm^{-1} may be assigned to $2\nu_2$ for the CO_3^{2-} ion (47). The symmetry of the CO_3^{2-} ion in the interlayer appears unperturbed (D_{3h}) relative to the free ion as no splitting of the CO_3^{2-} (ν_3) mode is observed and no ν_1 mode (expected at approximately 1050 nm) is detected. A weak, sharp peak at 1384 cm^{-1} is attributed to impurities of NO_3^- from the synthesis solution. Among the lattice vibrations an intense absorption around 336 cm^{-1} is observed for the Co(II)-Fe(III)-PTCs. Preliminary investigations show that a similar absorption, seems to be present in all PTCs. This absorption band resembles the band assigned to the E_u and A_{2u} lattice modes in brucite (48,49).

ACKNOWLEDGMENTS

REFERENCES

1. C. B. Koch and S. Mørup, Clay Miner. 26, 577 (1991).
2. S. Miyata, Clays Clay Miner. 31, 305 (1983).
3. T. Sato, T. Wakabayashi, and M. Shimada, Ind. Eng. Chem. Prod. Res. Dev. 25, 89 (1986).
4. G. A. O'Neil, C. Misra, and A. S. C. Chen, U.S. Patent 4,867,882 (1989).
5. G. A. O'Neil, J. W. Novak, and E. S. Martin, U.S. Patent 4,935,146 (1990).
6. A. Manabe and S. Miyata, U.S. Patent 4,458,030 (1984).
7. S. Miyata and T. Hirose, Clays Clay Miner. 26, 441 (1978).
8. F. Cavani, F. Trifirò, and A. Vaccari, Catal. Today 11, 173 (1991).
9. R. Allmann, Chimia 24, 99 (1970).
10. H. F. W. Taylor, Mineral. Mag. 39, 377 (1973).
11. R. Allmann, Acta Crystallogr. Sect. B 24, 972 (1968).
12. R. Allmann, N. Jahrb. Min. Mhft, 552 (1969).
13. R. Allmann and H. P. Jepsen, N. Jahrb. Min. Mhft., 544 (1969).
14. D. L. Bish, Bull. B. R. G. M. (deux. ser.), 293 (1978).
15. H. C. B. Hansen and R. M. Taylor, Clay Miner. 26, 311 (1991).
16. R. M. Taylor and R. M. McKenzie, Clays Clay Miner. 28, 179 (1980).
17. H. C. B. Hansen and R. M. Taylor, Clay Miner. 25, 161 (1990).
18. H. C. B. Hansen and R. M. Taylor, Clay Miner. 26, 507 (1991).
19. M. C. Gastuche, G. Brown, and M. M. Mortland, Clay Miner. 7, 177 (1967).
20. W. T. Reichle, Solid State Ionics 22, 135 (1986).
21. A. A. Olowe and J. M. R. Génin, Hyperfine Interact. 46, 445 (1989).
22. A. A. Olowe, D. Rezel, and J. M. R. Génin, Hyperfine Interact. 46, 429 (1989).
23. R. M. Taylor, Clays Clay Miner. 32, 167 (1984).
24. R. M. Taylor and U. Schwertmann, Clay Miner. 10, 299 (1974).
25. U. Schwertmann, Z. Anorg. Allg. Chem. 298, 337 (1959).
26. U. Schwertmann and H. Thalmann, Clay Miner. 11, 189 (1976).
27. T. Misawa, K. Hashimoto, and S. Shimodaira, Corros. Sci. 14, 131 (1974).
28. R. M. Taylor, Clay Miner. 15, 369 (1980).
29. J. D. Bernal, D. R. Dasgupta, and A. L. Mackay, Clay Miner. Bull. 4, 15 (1959).
30. W. Feitknecht, Helv. Chim. Acta 25, 555 (1942).
31. J.-C. Petit, C. R. Seances Acad. Sci. Ser. A. 251, 878 (1960).
32. D. Smith, M. C. Nichols, and M. E. Zolensky, "POWD10. A Fortran IV Program for Calculating X-Ray Powder Diffraction Patterns—Version 10." Pennsylvania State University, 1982.
33. D. J. Morgan, J. Therm. Anal. 12, 245 (1977).
34. W. Stumm and G. F. Lee, Ind. Eng. Chem. 53, 143 (1961).
35. H. C. B. Hansen, "Clay Minerals with Anion Exchange Properties. Synthesis and Characterization of Pyroaurite Group Double Metal Hydroxides containing Iron, Manganese or Chromium." Thesis, Chem. Dep., Royal Vet. & Agricult. University, Copenhagen, (1990). [In Danish]
36. A. C. C. Tseung and J. R. Goldstein, J. Mater. Sci. 7, 1383 (1972).
37. G. J. Ross and H. Kodama, Am. Mineral. 52, 1036 (1967).
38. P. G. Rouxhet and H. F. W. Taylor, Chimia 23, 480 (1969).
39. H. C. B. Hansen and C. B. Koch, in preparation.
40. M. A. Ulibarri, J. M. Fernandez, F. M. Labajos, and V. Rives, Chem. Mater. 3, 626 (1991).
41. E. C. Kruissink, L. L. Van Reijen, and J. R. H. Ross, J. Chem. Soc. Faraday Trans. 1 77, 649 (1981).
42. O. Clause, M. Gazzano, F. Trifirò, A. Vaccari, and L. Zatorski, Appl. Catal. 73, 217 (1991).
43. M. J. Hernandez, M. A. Ulibarri, J. L. Rendon, and C. J. Serna Thermochim. Acta 81, 311 (1984).
44. S. Miyata, Clays Clay Miner. 28, 50 (1980).
45. M. J. Hernandez-Moreno, M. A. Ulibarri, J. L. Rendon, and C. J. Serna, Phys. Chem. Miner. 12, 34 (1985).
46. C. J. Serna, J. L. White, and S. L. Hem, J. Pharm. Sci. 67, 324 (1978).
47. W. D. Bischoff, S. K. Sharma, and F. T. Mackenzie, Am. Mineral. 70, 581 (1985).
48. R. A. Buchanan, H. H. Caspers, and J. Murphy, Appl. Opt. 2, 1147 (1963).
49. S. M. Mitra, Solid State Phys. Adv. Res. Appl. 13, 1 (1962).